This is an author produced version of a paper published in
Scandinavian Journal of Forest Research.
This paper has been peer-reviewed but may not include the final publisher
proof-corrections or pagination.

Access to the published version may require journal subscription.
Published with permission from: Taylor & Francis.

Epsilon Open Archive http://epsilon.slu.se

Comparison between TanDEM-X and ALS based estimation of above ground biomass and tree height in boreal forests

Henrik J. Persson* and Johan E.S. Fransson

Department of Forest Resource Management, Swedish University of Agricultural Sciences, Umeå, Sweden;

*Author to whom correspondence should be addressed;

Henrik Jan Persson*, E-Mail: henrik.persson@slu.se, Tel.: +46-90-786-8105

Johan Erik Stefan Fransson, E-Mail: johan.fransson@slu.se , Tel.: +46-90-786-8531

Comparison between TanDEM-X and ALS based estimation of above ground biomass and tree height in boreal forests

Interferometric Synthetic Aperture Radar (InSAR) data from TanDEM-X were used to estimate above ground biomass (AGB) and tree height with linear regression models. These were compared to models based on airborne laser scanning (ALS) data at two Swedish boreal forest test sites, Krycklan (64°N19°E) and Remningstorp (58°N13°E). The predictions were validated using field data at stand-level (0.5 ha - 26.1 ha) and at plot-level (10 m radius). Additionally, the ALS metrics percentile 99 and vegetation ratio, commonly used to estimate AGB and tree height, were estimated in order to investigate the feasibility of replacing ALS data with TanDEM-X InSAR data.

Both AGB and tree height could be estimated with about the same accuracy at stand-level from both TanDEM-X and ALS based data. The AGB was estimated with 17.2% and 14.6% Root Mean Square Error (RMSE) and the tree height with 7.6% and 4.1% RMSE from TanDEM-X data at stand-level at the two test sites Krycklan and Remningstorp. The Pearson correlation coefficients between the TanDEM-X height and the ALS height p99 were r=0.98 and r=0.95 at the two test sites. The TanDEM-X height contains information related both to tree height and forest density, which was validated from several estimation models.

Keywords: TanDEM-X, InSAR, Forest, Biomass, Height, ALS, SAR

1. Introduction

Remote sensing is widely used for surveillance of forests on many scales. At a local and regional level, forest companies have invested significant resources in inventories to plan timber production in terms of pre-commercial thinning, thinning, final harvesting and reforestation. Remote sensing has also become crucial for national level monitoring and for development of comparative inventory methods between countries and continents. In the past, forest companies have used field visits and manual *in-situ* measurements to estimate forest variables such as basal area-weighted mean tree height and stem volume. Researchers and the global initiatives on the other hand, have been working with different remote sensing techniques for decades and today airborne laser scanning (ALS) is frequently used in commercial applications.

The tree height is often recognized as "Lorey's mean height", and the stem volume is approximately related to above ground biomass, AGB [tons ha^{-1}], through a scaling factor about 0.6 (Häme et al. 1992). ALS enables full coverage measurement of the forest structure and it can be used for creating digital terrain models (DTMs) to describe ground elevation. The estimations based on ALS data (especially the upper height percentiles, e.g., 95 and 99, denoted p95 and p99) are known to be efficient for estimation of tree height and related forest variables (Nilsson 1996; Reutebuch et al. 2003; Hyyppä et al. 2008; St-Onge et al. 2008). ALS metrics are also consistent throughout the measurements and have a higher precision than ordinary manual *in-situ* measurements, in which the tree height is commonly measured using a hypsometer. As a hypsometer is a hand held instrument even small movements can result in a variation of the measured tree height. ALS is therefore a reliable method to achieve complete site independent metrics (compared to sampled field plots that often use site dependent allometric equations to derive indirect variables such as AGB).

Stem volume and AGB (Eq. 1) are recognized as dependent on a combination of the vegetation height and the forest density (Treuhaft & Siqueira 2004).

$$AGB \propto vegetation\ height \cdot forest\ density \qquad (1)$$

In Hopkinson & Chasmer (2009), it was shown how ALS data strongly correlate (r^2=0.78) with canopy fractional cover. Furthermore, the vegetation ratio (VR) derived from ALS data has shown to be an efficient estimator of forest density and canopy cover and also for estimation of AGB (Hopkinson & Chasmer 2009; Nyström et al. 2012). Many studies have shown that one of the upper height percentiles (e.g., p95) in combination with the VR computed from ALS data can be used to estimate AGB and tree height with excellent accuracy (Næsset 2002; Næsset et al. 2004; Holmgren 2004; Næsset 2007).

Despite the unsurpassed accuracy of ALS data, it is inconvenient and relatively expensive to acquire, and therefore, equally good satellite based techniques could be an alternative to facilitate more frequent acquisitions at lower costs. Optical satellite sensors suffer from problems with cloud cover, which makes frequent acquisitions rare. Synthetic aperture radar (SAR) acquires images with an active technique and with wavelengths that overcome the problems associated with cloud cover. It has long been neglected within operational forest estimation due to its lack of necessary performance in terms of image resolution and also problems associated with signal saturation effects when estimating AGB from backscatter intensity at shorter wavelengths (Dobson & Ulaby 1992; Toan & Beaudoin 1992; Rignot et al. 1994; Imhoff 1995; Fransson & Israelsson 1999).

However, backscatter based models are not the only way of using SAR data and the last decade has seen a rapid development of different SAR based techniques. Since the late nineties and early 21st century, interferometric SAR has been investigated in different configurations. Interferometry uses phase differences between two acquisitions, and when

forests are considered, the coherence has been too low between two repeat-pass acquisitions to enable usage of the crucial phase information. A bi-static single-pass SAR configuration in space with high coherence was demonstrated with the Shuttle Radar Topography Mission (SRTM) orbiting the earth for 11 days in the year 2000, where space-borne C- and X-band data became available for over 80% of the globe. This proof-of-concept had one antenna mounted on the space shuttle, and a second antenna mounted on a 60 m long mast, extending from the shuttle. The derived InSAR products with approximately 30 m resolution in the X-band have been used to estimate forest height with a few meters root mean square error (RMSE; Simard et al. 2006; Solberg, Astrup, Bollandsa, et al. 2010).

With the launch of the German TanDEM-X satellites in 2007 and 2010 a new era began with high resolution X-band InSAR images with single- and dual-polarizations overcoming earlier problems with temporal decorrelation and low resolution, and hence offering applications at entirely new scales (Krieger et al. 2007; Martone et al. 2013). The interferometric SAR height (ISH; sometimes called scattering phase center height), contains combined information about both tree height and forest density, although intuitively directly relating to tree height. Consequently, the relationship to AGB could be direct, as discussed in Mette et al. (2004), Neeff et al. (2005), and Solberg et al. (2010; 2013). This also agrees well with the findings of Treuhaft & Siqueira (2004) who suggested that AGB is proportional to the product of vegetation height and forest density. Nevertheless, the weighting of respective component is still explored, for example, by using power law equations; *AGB $\propto$ height$^\alpha$* (Askne et al. 2013; Soja et al. 2015a; Torano Caicoya et al. 2015; Soja et al. 2015b).

Several studies have tried to isolate and evaluate the TanDEM-X ISH relation to tree height, as tree height is independent of the forest density. However, the ISH varies with phenology and species, which complicates comparisons between studies. The ISH can vary as much as 30% depending on frozen or unfrozen conditions and the dependence on species can

be 28% (3.4 m) in decidous forest and 17% (2.2 m) in coniferous forest throughout the year (Caicoya et al. 2012; Demirpolat 2012; L. M. H. Ulander et al. 2013; Kugler et al. 2014). Moreover, the penetration depends on leaf-on/off conditions (Praks, Hallikainen, et al. 2012; Praks, Antropov, et al. 2012; L.M.H. Ulander et al. 2013).

Few studies have investigated how TanDEM-X InSAR data (coherence and phase height) are influenced by forest density. Torano Caicoya et al. (2015) studied how classical allometric equations are affected by changing forest density and structure, using Legendre polynomials. Likewise, the interferometric coherence depends largely on volume (de-)correlation, which is influenced not only by the tree height but also forest structure. This has so far mainly been explored through inversion-based models, for example, the interferometric water cloud model, random volume over ground or the two-level model (Askne et al. 1997; Izzawati et al. 2006; Askne et al. 2013; Kugler et al. 2014; Torano Caicoya et al. 2015). However, Schlund et al. (2015) demonstrated how TanDEM-X coherence solely showed a moderate correlation with biomass ($R^2 = 0.5$) in a tropical peat swamp forest.

There are a limited number of TanDEM-X based studies that have evaluated its potential in boreal forests and more knowledge are needed. In short, TanDEM-X data have been used for AGB and stem volume estimations in studies with RMSEs about 12% to 33% at stand-level, and 32% to 40% RMSE at plot-level, (Solberg, Astrup, Gobakken, et al. 2010; Askne et al. 2013; 2013; Karila et al. 2015). Correspondingly, tree height has been estimated with about 1.5 to 2 m RMSE at stand-level and 3 to 5 m RMSE at plot-level (Praks, Antropov, et al. 2012; Kugler et al. 2014; Karila et al. 2015; Soja et al. 2015b).

The objectives of this study were to explore the potential of replacing ALS data with TanDEM-X InSAR data for operational use in the estimation of boreal forest variables. This included comparing estimation accuracies of AGB and tree height based on ALS data and TanDEM-X data, separately. Furthermore, the correspondence between TanDEM-X InSAR

data and the in forestry most important ALS metrics, height percentile 99 and vegetation ratio, was evaluated. Finally, the importance of forest density and its effect on AGB and tree height estimations was assessed through vegetation ratio and coherence metrics.

2. Material

2. 1 Field data

Two Swedish test sites with different site conditions were used (Figure 1). The first site was the Krycklan river catchment area located in northern Sweden (Lat. 64°16'N, Long. 19°46'E). The prevailing tree species were Scots pine (*Pinus sylvestris*; mainly in dry upslope areas), Norway spruce (*Picea abies*; mainly in wetter, low-lying areas), and birch (*Betula pendula* and *Betula pubescens*, in the riparian forest along larger streams). The region is hilly with elevations between 125 m and 350 m above sea level.
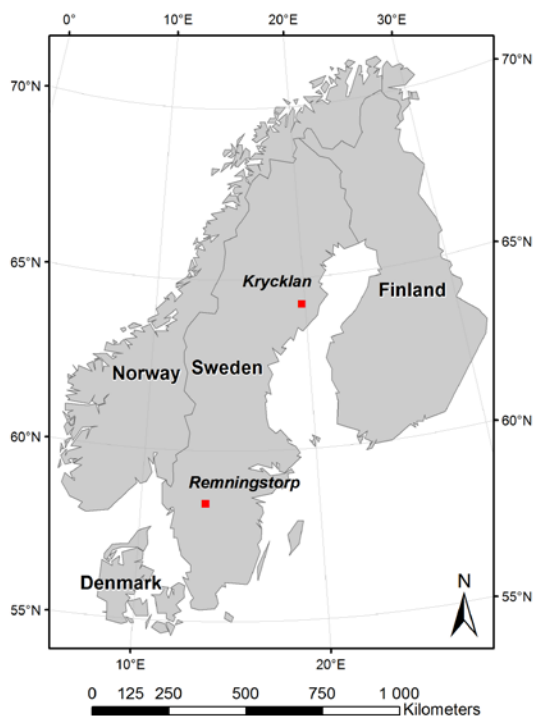
Figure 1. The two test sites Krycklan and Remningstorp, located in northern (64°N 19°E) and southern (58°N 13°E) Sweden, respectively.

In 2008 an extensive study was carried out on the Krycklan test site, where the field data used in the present study were collected during August – October (Hajnsek et al. 2009). These consisted of 31 stands with sizes varying between 2.4 ha and 26.1 ha. In the stands, field plots were distributed with a systematic spacing of 50 m to 160 m, depending on the size of the stand. The spacing in each stand was determined with the aim of obtaining 10 plots in each stand. The resulting number of plots for all stands varied between 8 and 13, with an average of 10 plots per stand. In total, 311 field plots were allocated within the 31 stands investigated. On the plots with 10 m radius, all trees with a diameter at breast height (DBH) ≥ 0.04 m were calipered and the species registered. On randomly selected sample trees (selected with the probability proportional to basal area) height and age were also measured using a hypsometer and a drill (Ducey 2009). On average, 1.5 sample trees were selected per plot. The AGB was computed using allometric equations and the heights were found using Söderberg's height functions (Söderberg 1986; Petersson 1999).

By observing SPOT-5 images, two stands were identified as clear-cuts and therefore removed, resulting in 29 forested stands. For the plot-level modeling at Krycklan, a subset of 29 plots was selected by randomly choosing one plot from each inventoried stand (Figure 2).
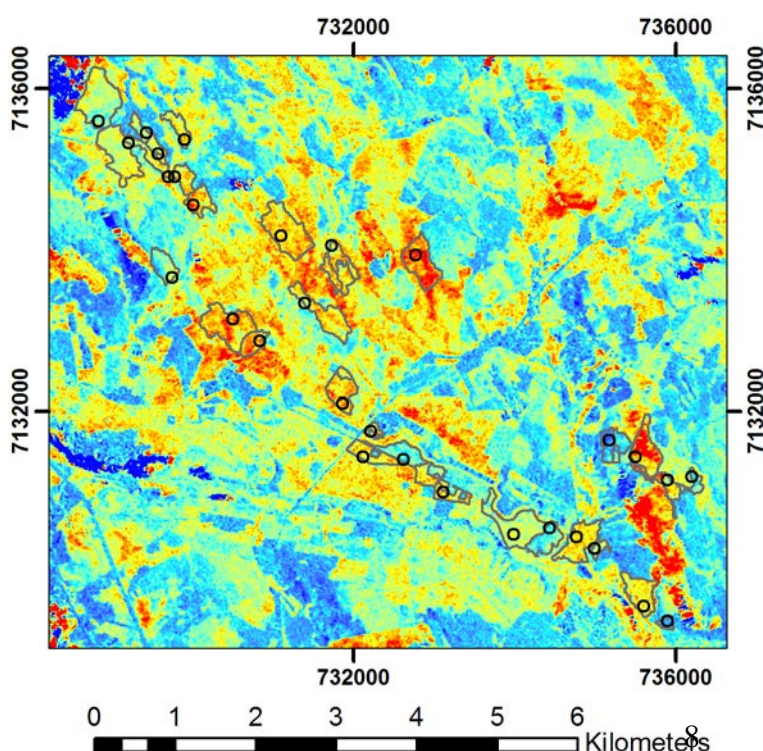
The statistics for the AGB and tree height estimates based on field data are listed in Table 1.

Figure 2. A TanDEM-X InSAR derived CHM with 29 forest stands and 29 field plots with 10 m radius delineated at Krycklan. The scale of the field plots is not correct.

Test site	Variable	Unit	Minimum	Mean	Maximum	Standard deviation
Krycklan	AGB	tons ha^{-1}	23	95	183	40
Krycklan	H	m	8	15	21	3
Remningstorp	AGB	tons ha^{-1}	55	155	284	50
Remningstorp	H	m	16	24	31	4

Table 1. AGB and tree height statistics for the test sites Remningstorp and Krycklan based on 32 and 29 stands, respectively.

The second test site, Remningstorp, is located in southern Sweden (Lat. 58°30'N, Long. 13°40'E), and comprises about 1,200 ha of productive forest land. The prevailing tree species were Norway spruce, Scots pine and birch. The dominant soil type is till (i.e., a mixture of glacial debris) with a field layer consisting of different forbs, bilberry (*Vaccinium myrtillus*) and grasses (e.g., *Deschampsia flexuosa*). In denser old spruce stands, the field layer is absent. It is a rather flat region with moderately varying ground elevations between 120 m and 145 m above sea level.

Field plot data for the Remningstorp test site were inventoried in the late fall of 2010 and in the early spring of 2011 (Ulander et al. 2010). All the plots were therefore completed after the 2010 vegetation season and before the 2011 vegetation season. In total, 32 field plots with 40 m radius were allocated over the estate at subjectively chosen locations (Figure 3). The main criteria were to locate the plots inside homogenous stands, large enough to hold a circular plot with 40 m radius, and also to reflect a wider range of stem volumes and forest types. Out of all possible stands fulfilling these criteria, the stands located the closest to roads were chosen for logistical reasons. Because of the size of these field plots, they were considered as small stands, 0.5 ha each. All trees with a DBH $\geq$ 0.04 m were calipered and positioned using a real time kinematic global positioning system. About 10% of the trees

were randomly selected and tree height measurements were undertaken using a hypsometer. Some additional trees were selected manually for height measurement to get a more even distributed set of measured heights without gaps. Young forest stands (< 25 years) were not chosen for this inventory as every tree had to be calipered and in young forests this can easily be several thousand stems ha^{-1}. The AGB for the 40 m plots were estimated using the Heureka forestry decision support system (Wikström et al. 2011). The exclusion of young stands increased the risk that the empirical modeling would become less generic and possibly biased, as the entire range of AGB and tree height was not represented.
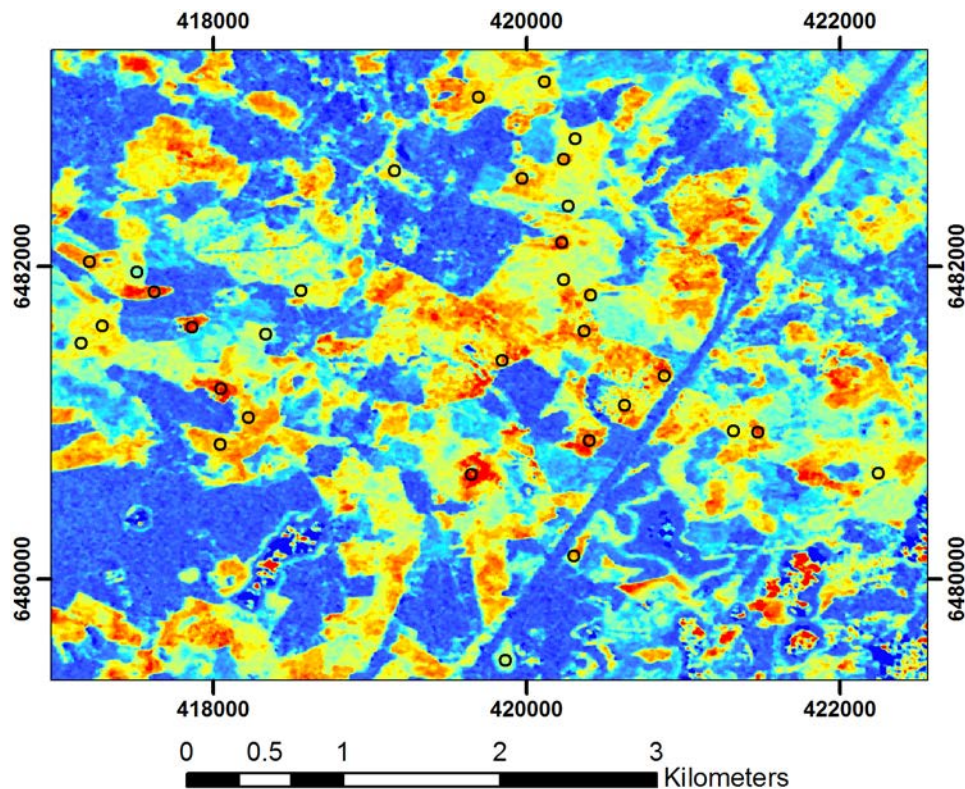
Figure 3. A TanDEM-X InSAR derived CHM with 32 forest stands consisting of 32 field plots with 40 m radius delineated at Remningstorp. The scale of the field plots is not correct.

A plot-level set for Remningstorp consisting of 32 plots with 10 m radius was established by choosing only the inner trees (within 10 m radius) in the previously described 32 field plots. The AGB for the 10 m plots were estimated using allometric equations and DBH as an input

variable (Marklund 1988). Correspondingly, the tree height was estimated for all calipered

trees on each plot (10 m radius) by using Equation 2, where h_i is the tree height and DBH_i is

the DBH of tree i before aggregating to plot-level in order to estimate tree height. α, $β_1$, and

$β_2$ are the regression coefficients.

$$\ln(h_i) = α + β_1\, DBH_i + β_2 \ln(DBH_i) \tag{2}$$

The RMSE and relative RMSE were used in order to describe the modeled error, and where

the latter simplifies comparisons between models using different units. The relative RMSE

was calculated using Equation 3, where $\hat{Y}_i$ and Y_i were the estimated and reference variables

(AGB or tree height) for stand i and n stands in total.

$$Relative\ RMSE = \frac{\sqrt{\sum_{i=1}^{n}(\hat{Y}_i - Y_i)^2/n}}{\sum_{i=1}^{n}(Y_i)/n}\,100 \tag{3}$$

All data sources were transformed to match the Swedish reference frame 1999 Transverse

Mercator (SWEREF99TM) that is based on UTM-33N/WGS84 (covering most of Sweden)

and then extended to the adjacent UTM zones (32 and 34) in the western and eastern parts.

2. 2   ALS data

At the Krycklan test site, the ALS data were scanned October 13, 2010, and provided by the

Swedish National Land Survey (Lantmäteriet) through the project "Ny Nationell

Höjdmodell" ("New National Elevation Model"). This project commenced in 2009 and is

expected to be finished by 2016 (Bergström et al. 2009; Lundgren & Juni 2010). The goal is

to scan the whole of Sweden in order to generate an accurate DTM which, as only minor

changes in the terrain are expected, should remain stable for the foreseeable future. The ALS

data were collected with at least 0.5 returns m^{-2} at a laser wavelength of 1064 nm, and were

used as above ground ALS reference data in Krycklan. These ALS data were also used to

create DTMs as reference for both test sites and the height reference system was Rikets Höjdsystem 2000 (RH2000) (Svensson et al. 2006).

The ALS of the Remningstorp estate was performed on August 29 and September 9, 2010, with a laser wavelength of 1550 nm and at least 10 returns m^{-2} from 400 m altitude and at least 30 returns m^{-2} from 200 m altitude above ground level (Ulander et al. 2010).

2.3   TanDEM-X data

The dual-pol TanDEM-X data image pairs were both acquired in June 2011, in strip-map (SM) mode with a single-pass bi-static right-looking configuration from ascending orbits. They were delivered as co-registered Single Look Complex (SLC) data in CoSSC format. The VV polarization was chosen over the VH, as considerably more stable scattering phase center heights were attained in forest regions and with subsequent more accurate interferometric height models as result. The VV polarization is known to penetrate slightly less than the HH channel in boreal forests (Perko et al. 2011; Demirpolat 2012; Kugler et al. 2014). The ALS data were acquired for the two test sites slightly earlier than the radar data, but mainly within the same vegetation season. Moreover, the ALS estimates are rather consistent, in both leaf-on and leaf-off conditions and especially in coniferous forests (Wasser et al. 2013). For Krycklan and Remningstorp, the TanDEM-X image pairs were acquired during the summer of 2011, with a mean scene center incidence angle of 41° (Table 2). Steep incidence angles decrease the height sensitivity and increases the penetration depth (Kugler et al. 2014). The authors' experience agree with this fact and we think incidence angles in the range of 30° to 50° are most suitable for forest applications. The weather conditions at both test sites were dry at the time for the acquisitions with no precipitation the previous 24 hours (Table 2).

The height of ambiguity (HOA) is related to the baseline and affects the height sensitivity of an interferometer. It describes the altitude difference that generates an

interferometric phase change of 2π, which also means, that no phase unwrapping errors could appear when the objects measured are smaller than the HOA. Therefore, HOA gives a measure of the image pair's suitability for tree height estimations and is defined as (Eq. 4):

$$HOA = \frac{2\pi}{k_z} = \frac{\lambda R \sin\theta}{B_\perp}$$

(4)

where k_z is the vertical wave number, λ is the radar wavelength, R is the average distance to the satellites, θ is the average angle of incidence and $B_\perp$ is the perpendicular baseline. The image data characteristics and test site conditions are summarized in Table 2.

Test Site	Date	Polarization	Resolution Range/Azimuth (m)	Mode	Inc. Angle (°)	HOA (m)	Precipitation (mm)	Temp (°)
Krycklan	2011-06-17	VH/**VV**	1.8/6.6	SM	41	52	0	13.6
Remningstorp	2011-06-04	VH/**VV**	1.8/6.6	SM	41	49	0	18.8

Table 2. TanDEM-X data characteristics and test site conditions during acquisition. The polarization used is marked in bold.

3. Methods

3. 1   ALS processing

The raw ALS point clouds were processed using Lastools (Isenburg). First, a ground classification was performed to be able to construct a ground triangulated irregular network. Thereafter, the height for each individual ALS point was computed. Finally, rasters were created for the height percentiles 10 to 100 (denoted p10, p20 …, p100) in 10% steps for each pixel and also for p95, p99 and vegetation ratio (VR). The output rasters were given a 5 m

pixel size. The percentiles were calculated using all returns above a height threshold of 1.37 m (software default and suitable for Swedish forest), which was used to avoid vegetation under the tree layer, which otherwise could influence the height distribution of returns. The VR was defined as the number of ALS returns from the vegetation above the height cutoff divided by the number of all ALS returns (Eq. 5, Morsdorf et al. 2006).

$$VR = \frac{\sum Returns_{vegetation}}{\sum Returns_{total}} \tag{5}$$

with (Eq. 6)

$$(\boldsymbol{Returns_{vegetation}} > 1.37 \text{ m}) \subset Returns_{total} \tag{6}$$

where $\boldsymbol{Returns_{vegetation}}$ and $Returns_{total}$ denotes vegetation returns and all (ground and vegetation) returns, respectively.

3.2   *InSAR processing*

The radar images (SLC data) were, together with an ALS based DTM, processed to interferometric SAR height (ISH) images using the Gamma software (Gamma). A digital surface model (DSM) was computed from the radar data and then the DTM was subtracted to attain the ISH, from which metrics were extracted to be used in the estimations of AGB and tree height. The DTM was attained as orthometric height and therefore, it was converted to ellipsoidal height using geoid heights obtained from Lantmäteriet.

The SLCs were already co-registered and, therefore, a geocoding look-up table (LUT) was computed for the coordinate transformation between the range-Doppler coordinates (RDCs) and orthonormal map coordinates. An initial transformation was calculated based on the orbital data and ancillary SAR image information. The ellipsoidal DTM was used as an orthonormal map reference and in this step a simulated SAR intensity image was generated

out of the DTM. The LUT was used to transform the simulated SAR intensity image into RDCs so that it could be used for refining the initial LUT. This was done by using cross-correlation analysis between a multilooked (ML) TanDEM-X image and the simulated SAR intensity image in RDCs. The planar registration offsets (difference between the images) were determined automatically and this procedure was iterated twice with a tighter threshold each iteration in order to achieve as good a transformation as possible. The multilooking used was 4 in range and 2 in azimuth, implying a rectangular ML pixel size of 5.6 m × 5.8 m in ground range and azimuth.

The two SAR images (expressing the ground reflectivity function of the scene) in an interferometric system can be processed to produce an interferogram, which is obtained from the Hermitian product of the two complex SAR images (Hagberg et al. 1995). This is the product of the first image and the complex conjugate of the second image (Eq. 7):

$$\tilde{\gamma} = s_1 s_2^* = \left(a_1 e^{-j\varphi_1} e^{-j\frac{4\pi}{\lambda}R_1}\right)\left(a_2 e^{-j\varphi_2} e^{-j\frac{4\pi}{\lambda}R_2}\right)^* \tag{7}$$

where s_1 and s_2 are the master and slave images, expressed in terms of their amplitudes, a_1 and a_2, and their phases, φ_1 and φ_2. R_1 and R_2 are the respective distances from the antenna to the ground. In practice, the interferogram was estimated from a finite number of samples through coherent averaging (Bamler & Hartl 1998; Hanssen 2001). We defined the measure of change between the two SLC images as the coherence $\tilde{\gamma}$, which also is called the complex correlation coefficient (Eq. 8):

$$\tilde{\gamma} = \frac{E[s_1 s_2^*]}{\sqrt{E[|s_1|^2]E[|s_2|^2]}} \tag{8}$$

where E[] are the expectation values (Bamler & Hartl 1998; Ferretti et al. 2007; Lee & Pottier 2009). The images were stored in RDCs to facilitate coherent multilooking. Subsequently the

coherence, defined as the magnitude of the cross-product of the two SLCs, was computed as $\gamma = |\widetilde{\gamma}|$.

To create the ISH phase map as DSM-DTM, (i.e., the range related phase of the DSM minus the range related phase of the scatterers at zero height on its topography), the DTM phase was computed from the ellipsoidal DTM using the orbit state vectors for baseline calculation. The DTM was resampled into RDCs using the LUT. Finally, the DTM was subtracted from the complex interferogram.

The resulting phase map was unwrapped using the minimum cost flow algorithm (Costantini 1998; Wegmüller et al. 2002). Because the terrain variations are smaller than the HOA (49 m and 52 m) in the image pairs used, no unwrapping was really necessary, but the MCF function made it convenient to shift the phases to get correct zero-height values for bare-ground regions.

For Krycklan, residual phase trends were still visible after unwrapping (possibly arising from an inadequate linear baseline model) and these were removed by fitting Equation 9 to the open regions in the image, found automatically from a mask generated from the coherence values greater than 0.7:

$$\Delta\varphi = \alpha_0 + \alpha_1 RG + \alpha_2 AZ \tag{9}$$

where $\Delta\varphi$ is an interception phase shift, α_0, α_1, and α_2 are correction factors and RG and AZ are the range and azimuth coordinates, respectively.

Finally, the remaining unwrapped phases were converted into ISHs and transformed (geocoded) to map geometry with 5 m pixel size using the LUT previously derived. Correspondingly the coherence maps were geocoded using the same LUT. Examples of the ISHs compared to ALS data and aerial photographs (ortho-photos) are illustrated in Figure 4.
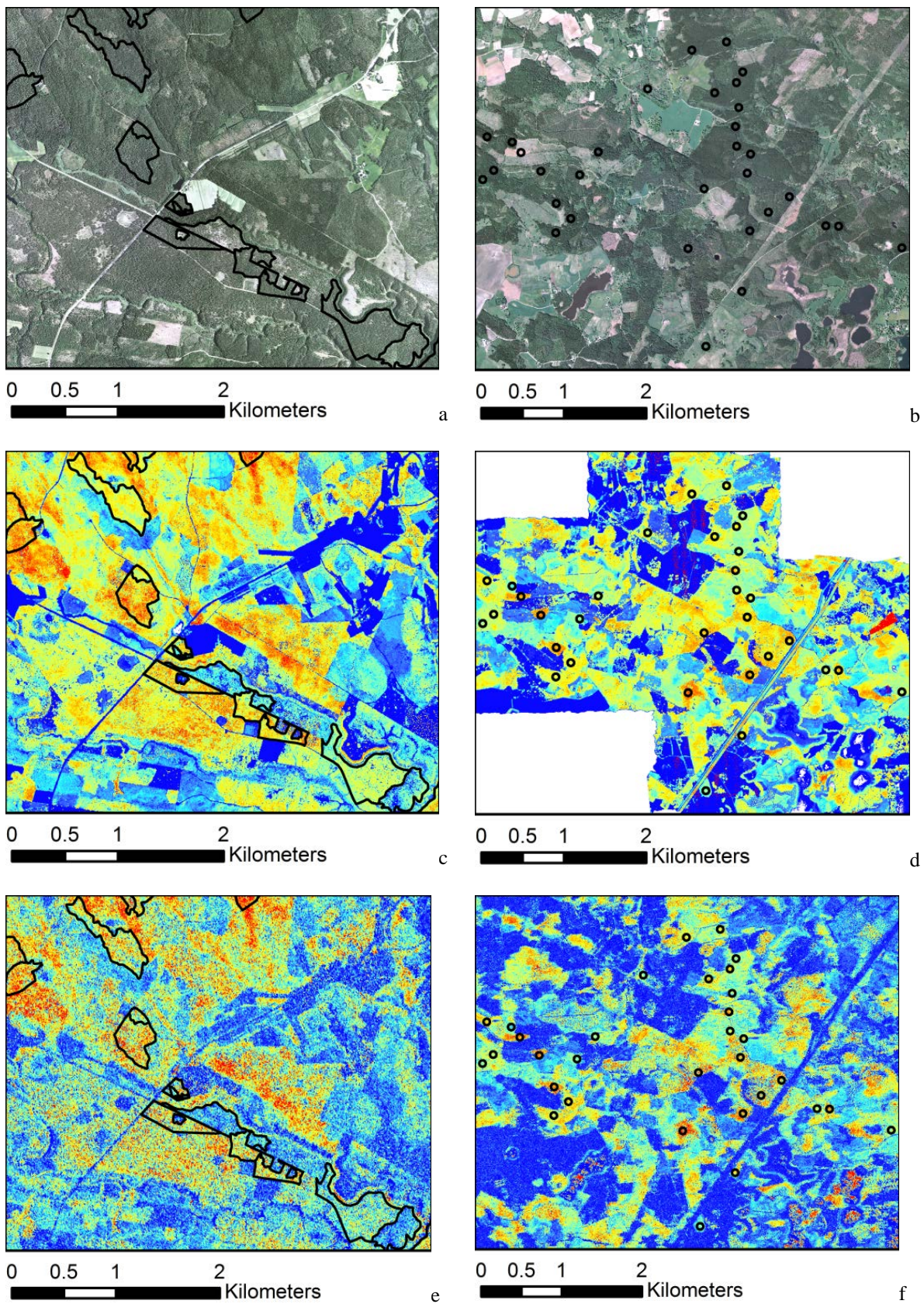
Figure 4. A selective clip from Krycklan (a, c, e) and Remningstorp (b, d, f). From top to bottom, the comparison between an ortho-photo (a, b), ALS p99 (c, d) and TanDEM-X derived ISH (e, f) are illustrated.

3.3   Statistical modeling

For each test site, SAR metrics (mean ISH and mean coherence) and correspondingly the ALS metrics described in section 3.1 were extracted at stand- and plot-level. Linear regression was used for estimation of the AGB and tree height. A short, still accurate, empirical model was found based on ALS data using the metrics p99, p60 and VR. The metrics p99 and VR were clearly most important, intuitively straightforward, and relevant to other studies, and therefore it was decided to use these as ALS reference data. Hence, AGB, tree height, p99, and VR were modelled from the InSAR data. This included testing of both the previously named conceivable height and density metrics, but also their combinations and transformations. ISH was the only metric that become significant in its transformed form, ISH^2, and no values of the exponent less than 1 or exceeding 2 indicated any improvement over the selected values. For comparison to InSAR data, the AGB and tree height modeled using ALS data were used. The explanatory variables included in the regression models were selected with regards to their significance and their contribution to lowering the RMSE. For each model, residual plots were inspected and the degree of variance explanation was computed as the adjusted coefficient of determination (R^2_{adj}). The AGB and tree height were modeled with the TanDEM-X and ALS data at both stand-level (considering the 0.5 ha field plots with 40 m radius in Remningstorp as "stands") and plot-level (10 m radius). The models were evaluated using leave-one-out cross-validation, resulting in RMSE and relative RMSE values. The leave-one-out method used a single sample from the original data set for validation of a model trained using all other samples in the original data set. This was repeated so that each observation in the data set was used once for validation.

An example of the full model for estimating AGB from TanDEM-X data at stand-level is illustrated by:

$$AGB = \beta_0 + \beta_1 ISH + \beta_2 ISH^2 + \beta_3 COH \tag{10}$$

where $\beta_{0..3}$ are the regression coefficients, *ISH* is the mean *ISH*, and *COH* is the mean coherence.

Linear regression models describing the AGB and tree height were developed first with TanDEM-X InSAR data as explanatory variables and then with ALS data for comparison. TanDEM-X data were also used to estimate the ALS parameters p99 and VR. Models were created at stand- and plot-level and all models were developed so that the included parameters (except the intercept) were significant.

The significance was studied using the Student's *t*-test, which evaluates the hypothesis that the expectation value of the normally distributed parameter estimate $\hat{\beta}$ is β_i. The *t*-statistic was computed as:

$$t = \frac{\hat{\beta} - \beta_i}{\hat{\sigma}_{\beta_i}} \tag{11}$$

where $\hat{\sigma}_{\beta_i}$ is the estimated standard deviation of $\hat{\beta}$. The Student's *t*-test was used to test the hypothesis that $\beta_i = 0$. For a known number of degrees of freedom, the probability *p* of obtaining a certain *t*-statistic can be computed from the *t*-distribution. The significance levels were defined as; *** $= p \leq 0.001$, ** $= p \leq 0.01$, * $= p \leq 0.05$, ● $= p \leq 0.10$, and ns = non-significant.

4. Results

The evaluated models are listed in Table 3 with their corresponding parameters and significance levels. The results are presented in Sections 4.1-4.3 and in Tables 4-9, where the presented model numbers correspond to the models listed in Table 3.

Estimated variable	Test site	Model	Intercept β_0	ISH β_1	ISH^2 β_2	COH β_3	p99	p60	VR	Data source
AGB stand-level	KR	1	-61.8 ***		0.24 ***					SAR
	RE	2	-419 ***	14.6 ***		237 ***				SAR
	KR	3	-81.3 ***				5.96 ***		1.77 ***	ALS
	RE	4	-330 ***				7.86 ***		4.25 ***	ALS
H stand-level	KR	5	-0.653 ns	0.896 ***		-10.7 *				SAR
	RE	6	-1.09 ns	1.00 ***		-7.82 ***				SAR
	KR	7	4.90 ***				1.85 ***	-1.14 *	-0.0772 *	ALS
	RE	8	1.99 ●				0.995 ***			ALS
p99 stand-level	KR	9	-21.9 ***	2.33 ***	-0.0251 **	-10.2 ***				SAR
	RE	10	1.84 ns	0.906 ***		-11.4 ***				SAR
VR stand-level	KR	11	-23.5 ns		0.0607 ***	51.6 ●				SAR
	RE	12	11.2 ns		0.0257 ***	66.2 ***				SAR
AGB plot-level	KR	13	-167 ***	9.88 ***						SAR
	RE	14	-1470 *	87.9 *	-1.20 *	136 *				SAR
	KR	15	-57.2 ***				6.53 ***		1.14 *	ALS

	RE	16	-286 ***				5.28 **		4.81 ***	ALS
H plot-level	KR	17	4.41 ns	0.720 ***		-12.8 *				SAR
	RE	18	15.0 ***		0.0123 ***	-8.41 **				SAR
	KR	19	40.8 ***				9.81 ***		-0.762 *	ALS
	RE	20	2.00 *				0.982 ***			ALS

Table 3. Regression model parameters used for estimation of AGB and tree height at the test sites Krycklan (KR) and Remningstorp (RE). The significance levels (symbolized below the parameter values) were defined as; *** = $p \leq 0.001$, ** = $p \leq 0.01$, * = $p \leq 0.05$, ● = $p \leq 0.10$, and ns = non-significant.

4. 1 Estimation of AGB and tree height at stand-level

The TanDEM-X InSAR based estimations of AGB were similarly accurate at stand-level as the ALS based estimations (Table 4). The models were linear at both test sites within their respective ranges (23 to 183 tons ha^{-1} in Krycklan and 55 to 284 tons ha^{-1} in Remningstorp) and from the scatter plots (Figure 5 and 6) no tendency to saturation could be noted. In absolute terms, the error was higher at the Remningstorp test site when compared to Krycklan (22.2 tons ha^{-1} vs. 16.2 tons ha^{-1}), but as the mean AGB in Remningstorp was also higher, the results relative each other in relative terms were reversed (17.2% RMSE in Krycklan and 14.6% in Remningstorp; Table 4). The higher absolute error in Remningstorp indicates that either the field data were less accurate or that the forest structure and tree heights play an important role for the X-band penetration and therewith the estimation potential. The lower and also sparser forest in Krycklan could possibly be better suited to the X-band data for estimation of AGB (Table 4).

The AGB was modeled simply as a function of the ISH^2 in Krycklan while the model for Remningstorp could describe the AGB with the lowest relative RMSE by using both the ISH and the coherence as explanatory variables. This modeling difference restricts the transferability to other test sites and depends most likely on the different forest structures at the two test sites. The dynamic range of coherence was smaller in Krycklan than Remningstorp, which possibly made this not significant as explanatory variable. Remningstorp has denser forest which is mainly spruce dominated. The coherence contribution for AGB estimation in Remningstorp was considerable, and added almost 22% in the explanation of the variance in the data, R^2_{adj}.

The ISH was linearly correlated to the tree height and the coherence also became statistically significant for the explanation of tree height. The linear relationship held for the entire evaluated range of tree height at both test sites (8 to 21 m in Krycklan and 16 to 31 m in Remningstorp). The TanDEM-X InSAR data could explain 90% of the variance in Krycklan and 95% in Remningstorp (Figure 5 and 6). Furthermore, the tree height estimation error was 7.6% in Krycklan and 4.1% in Remningstorp (Table 5). This means that tree height estimation could be achieved slightly better with TanDEM-X InSAR data than with ALS data at stand-level in Remningstorp. Both the InSAR based and ALS based estimations had an RMSE about 1.0 m, which was close to the TanDEM-X specified local DEM accuracy of 0.8 m (Hajnsek et al. 2010) and only 1/3 of the relative 90% DEM height error (3.2 m) presented for agricultural areas in Rizzoli et al. (2012).

Test site	Technique	Date	R^2_{adj}	RMSE (tons ha^{-1})	RMSE (%)	No. of stands	Model no.
Krycklan	InSAR	2011-06-17	0.85	16.2	17.2	29	1
Remningstorp	InSAR	2011-06-04	0.81	22.6	14.6	32	2
Krycklan	ALS	2010-10-13	0.87	15.1	16.1	29	3
Remningstorp	ALS	2010-08-29	0.84	21.1	13.7	32	4

Table 4. Estimation of AGB from TanDEM-X InSAR and ALS data at stand-level.

Test site	Technique	Date	R^2_{adj}	RMSE (m)	RMSE (%)	No. of stands	Model no.
Krycklan	InSAR	2011-06-17	0.90	1.1	7.6	29	5
Remningstorp	InSAR	2011-06-04	0.95	1.0	4.1	32	6
Krycklan	ALS	2010-10-13	0.92	1.0	6.5	29	7
Remningstorp	ALS	2010-08-29	0.94	1.05	4.4	32	8

Table 5. Estimation of tree height from TanDEM-X InSAR and ALS data at stand-level.

4. 2   *Estimation of ALS p99 and VR at stand-level*

For estimation of ALS p99, the ISH together with the coherence were the most important explanatory variables (Table 3). The ISH was strongly correlated to ALS p99 at both test sites with Pearson correlation coefficients $r = 0.98$ and $r = 0.95$ for Krycklan and Remningstorp, respectively. The TanDEM-X InSAR data could explain 98% of the variance ($R^2_{adj} = 0.98$; Table 6) at both test sites. The RMSE was slightly lower when TanDEM-X InSAR data were used to estimate ALS p99 instead of tree height (Table 6 vs. Table 5),

which could possibly be connected to the fact that both InSAR and ALS originate from remote sensing techniques (in comparison to field measured calipered trees). A robust and consequent estimation of the ALS p99 variable is vital for a reliable replacement of ALS data. VR is a forest density metric and especially important for AGB estimations. VR could be estimated with 13.7% and 6.2% RMSE at the two test sites (Table 7). The squared ISH was the most important explanatory variable but especially in Remningstorp, the coherence also played an important role (Table 4).

Test site	Date	R^2_{adj}	RMSE (m)	RMSE (%)	No. of stands	Model no.
Krycklan	2011-06-17	0.98	0.7	4.8	29	9
Remningstorp	2011-06-04	0.98	0.6	2.7	32	10

Table 6. Estimation of ALS p99 from TanDEM-X InSAR data at stand-level.

Test site	Date	R^2_{adj}	RMSE	RMSE (%)	No. of stands	Model no.
Krycklan	2011-06-17	0.63	7.0	13.7	29	11
Remningstorp	2011-06-04	0.71	4.5	6.2	32	12

Table 7. Estimation of ALS VR from TanDEM-X InSAR data at stand-level.

4. 3   *Estimation of AGB and tree height at plot-level*

For the smaller sample plots with 10 m radius, the RMSE generally increased both in relative and absolute terms in comparison to the stand-level results. The TanDEM-X based models of AGB at plot-level resulted in about 50% higher RMSE at Krycklan and about twice the RMSE at Remningstorp when compared to the stand-level models (Table 8 vs. Table 4). The TanDEM-X InSAR data could explain 81% of the variance at Krycklan, which corresponds to approximately the same R^2_{adj} as at stand-level. This means that the InSAR model performs equally well as the model using ALS data at Krycklan. At Remningstorp the situation differs at plot-level to a greater extent when compared to the stand-level results. The

TanDEM-X InSAR data could explain 34% of the variance for AGB compared to 81% at stand-level and the absolute RMSE has more than doubled from 22.6 tons ha^{-1} at stand-level to 54.9 tons ha^{-1} at plot-level. The plot-level model using ALS data has also a higher RMSE (39.5 tons ha^{-1} or 20.5%) compared to the stand-level results (21.1 tons ha^{-1} or 13.7%). In relative terms, at Remningstorp, the InSAR errors for AGB were about twice as high at plot-level compared to stand-level while the ALS models were about 50% poorer.
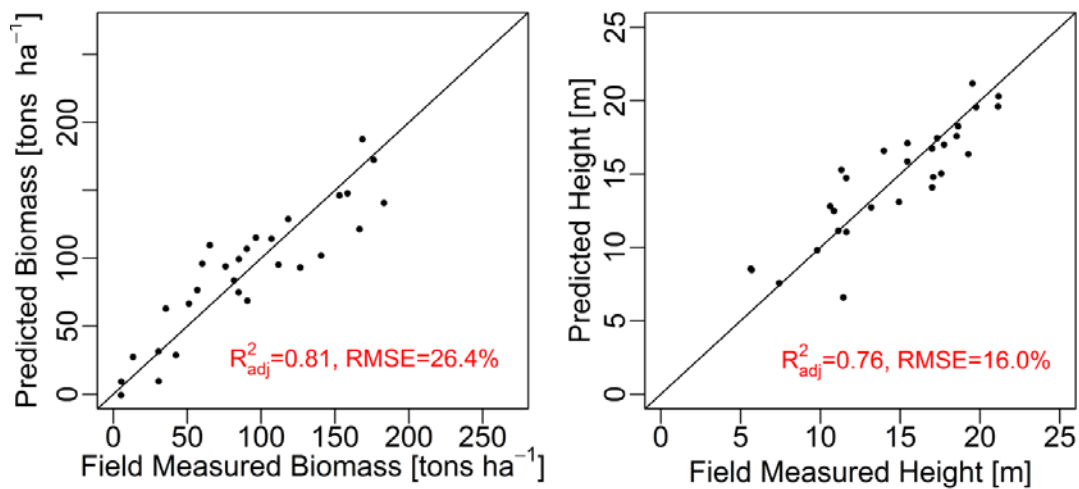
Figure 5. Scatter plots of AGB (left) and tree height (right) estimations at stand-level in Krycklan from TanDEM-X InSAR data.
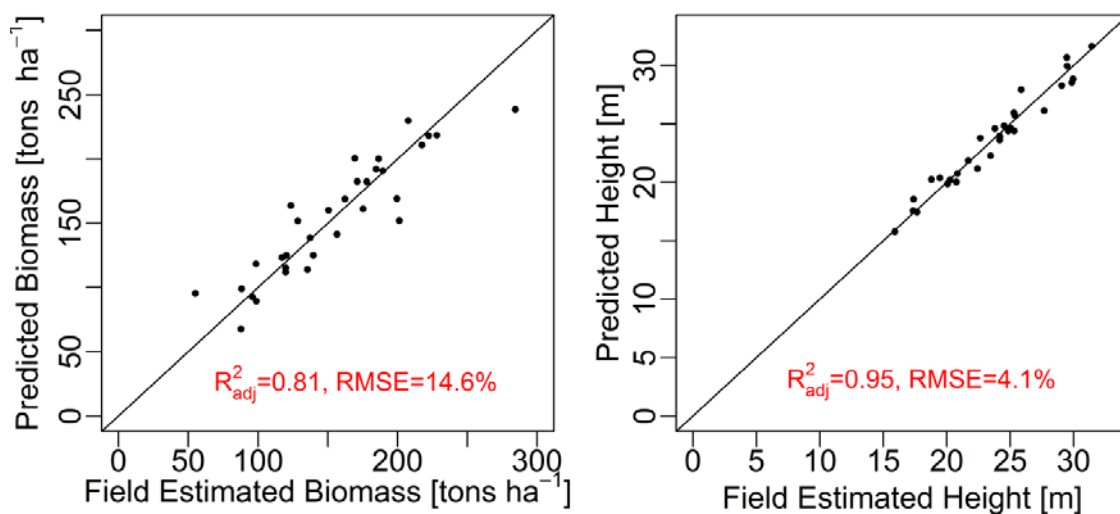

Figure 6. Scatter plots of AGB (left) and tree height (right) estimations at stand-level in Remningstorp from TanDEM-X InSAR data.
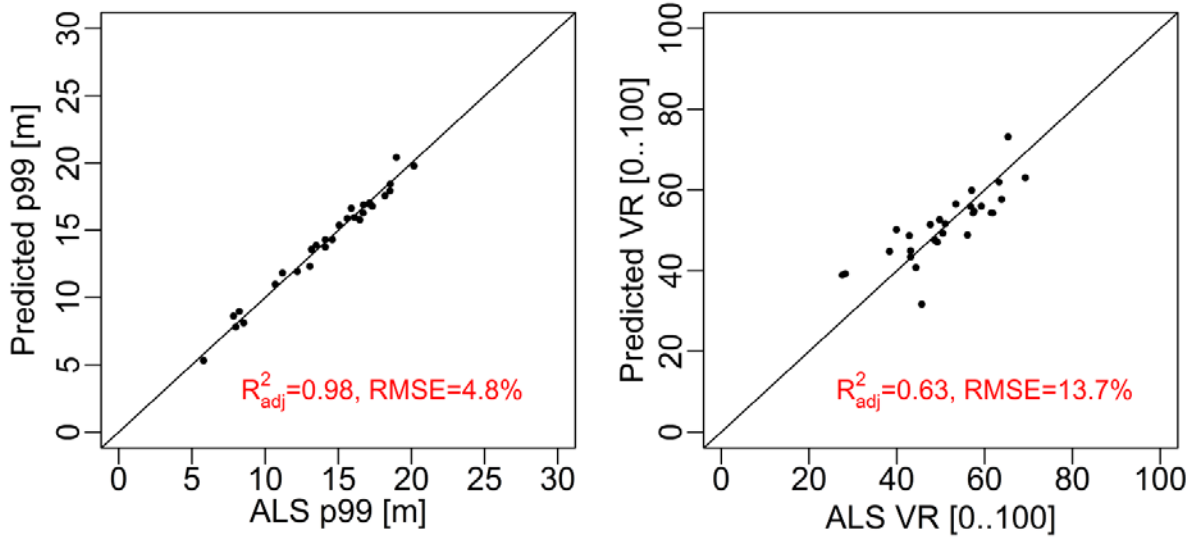
Figure 7. Scatter plots of ALS p99 (left) and ALS VR (right) estimations at stand-level in Krycklan from TanDEM-X InSAR data.
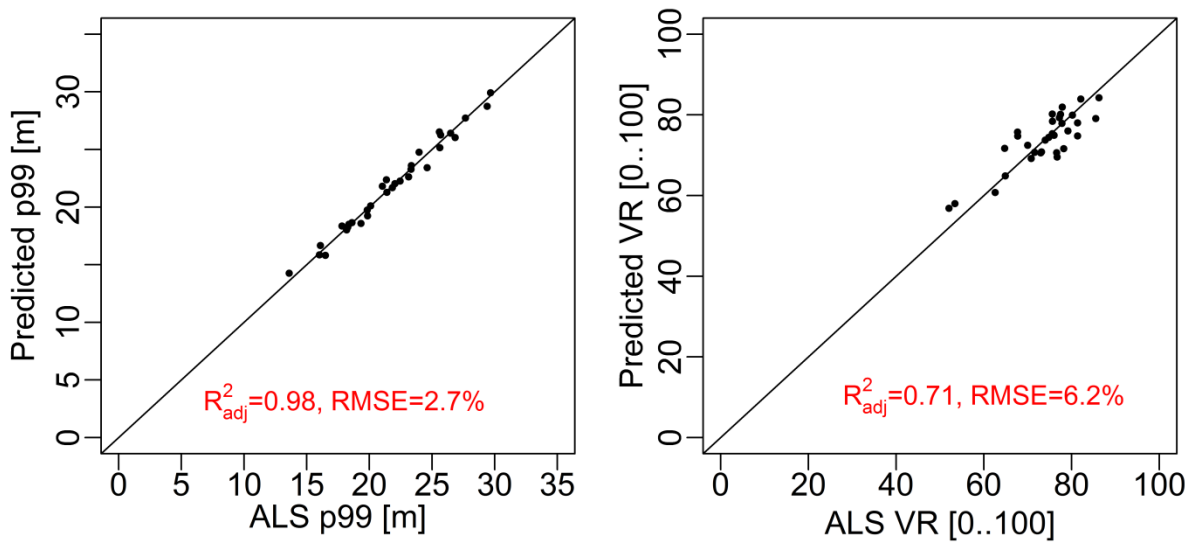

Figure 8. Scatter plots of ALS p99 (left) and ALS VR (right) estimations at stand-level in Remningstorp from TanDEM-X InSAR data.
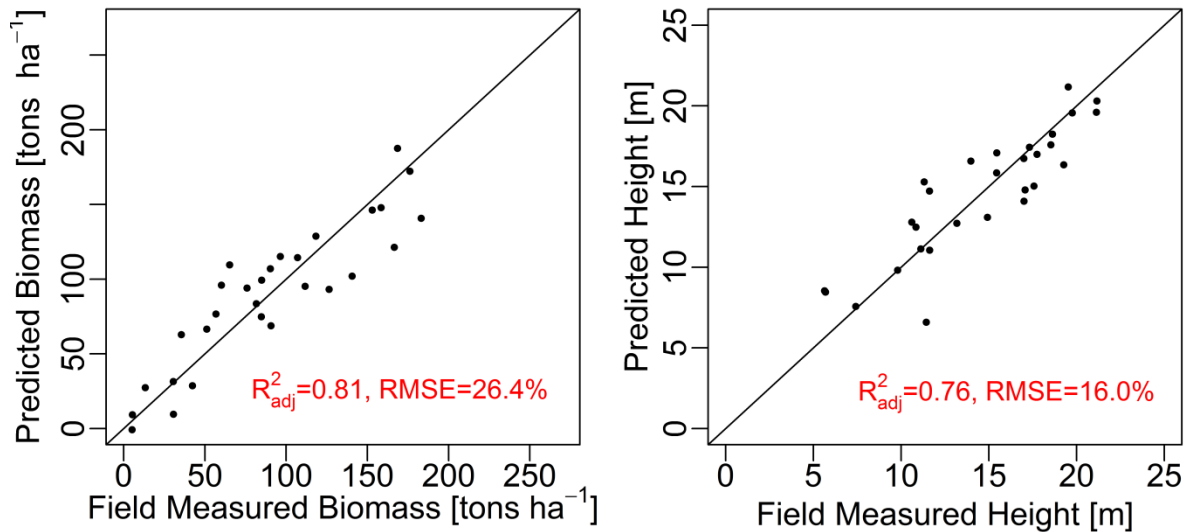
Figure 9. Scatter plots of AGB (left) and tree height (right) estimations of 29 field plots with 10 m radius in Krycklan using TanDEM-X InSAR data.
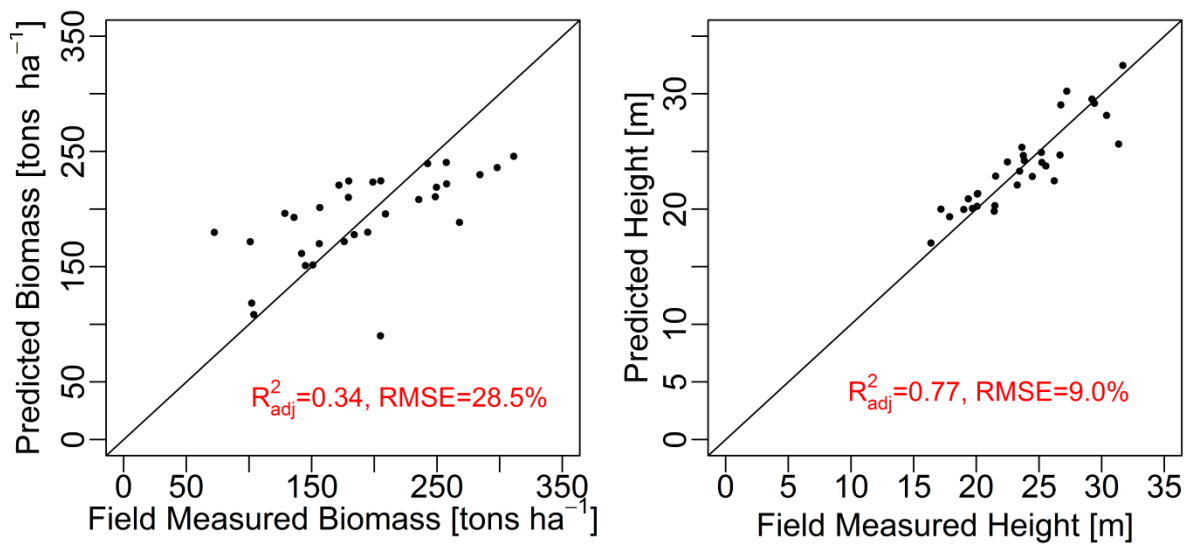

Figure 10. Scatter plots of AGB (left) and tree height (right) estimations of 32 field plots with 10 m radius in Remningstorp using TanDEM-X InSAR data.

The tree height estimations were influenced to a lesser extent by the smaller plot sizes compared with the stand-level results. In the case of InSAR, the RMSE was approximately the same for both test sites (2.3 m and 2.1 m, Table 9) and the data variance could be explained to 77%. This means that the error was about twice as large at plot-level compared

to stand-level even in relative terms (16.0% to 7.6% and 9.0% to 4.1%, respectively) for both test sites. The tree height models using ALS data (Table 9) showed results that are in line with those at stand-level (Table 5) in absolute terms (about 1 m RMSE) and in relative terms. The error for Krycklan increased from 6.5% to 9.6% while for Remningstorp it was exactly the same as at the stand-level (4.4%).

Test site	Technique	Date	R^2_{adj}	RMSE (tons ha^{-1})	RMSE (%)	No. of plots	Model no.
Krycklan	InSAR	2011-06-17	0.81	23.8	26.4	29	13
Remningstorp	InSAR	2011-06-04	0.34	54.9	28.5	32	14
Krycklan	ALS	2010-10-13	0.84	22.4	24.9	29	15
Remningstorp	ALS	2010-08-29	0.63	39.5	20.5	32	16

Table 8. Estimation of AGB from TanDEM-X InSAR and ALS data at plot-level with 10 m radius.

Test site	Technique	Date	R^2_{adj}	RMSE (m)	RMSE (%)	No. of plots	Model no.
Krycklan	InSAR	2011-06-17	0.76	2.3	16.0	29	17
Remningstorp	InSAR	2011-06-04	0.77	2.1	9.0	32	18
Krycklan	ALS	2010-10-13	0.91	1.4	9.6	29	19
Remningstorp	ALS	2010-08-29	0.95	1.0	4.4	32	20

Table 9. Estimation of tree height from TanDEM-X InSAR and ALS data at plot-level with 10 m radius.

5. Discussion

The purpose of this study was to explore the potential of replacing ALS data with TanDEM-X InSAR data for operational forestry use. The high resolution of TanDEM-X imagery acquired at suitable baselines resulted in good results for the respective model estimations, and at stand-level the results indicate a similar potential for TanDEM-X as ALS as a data source. For the two test sites evaluated in this study, it was possible to accurately model the AGB with a function of the ISH and/or its squared version, ISH^2, together with coherence. The AGB could be estimated at stand-level with somewhat lower RMSE of about 17% at Krycklan and 15% at Remningstorp when compared to other studies (Solberg, Astrup, Gobakken, et al. 2010; Askne et al. 2013; Solberg et al. 2013) that have reached about 17% to 20% RMSE in their correspondent best-cases using X-band InSAR data. In (2015a), they estimated the AGB with 12% to 19% RMSE using the same test sites (Remningstorp and Krycklan), however, the only image pair that led to higher estimation accuracy of AGB in Soja et al. (2015a), has not been evaluated in the present study. Their focus was on the presentation of a new semi-empirical scattering model, originating in physical scattering theory. Semi-empirical models were also applied in Askne et al. (2013), Kugler et al. (2014), and Soja & Ulander (2013). It is therefore interesting to see that simple empirical regression models can perform well and deliver results within the same order of magnitude as more complex semi-empirical models.

Considering the estimation of tree height at stand-level, it is remarkable that at Remningstorp it could be estimated with a lower RMSE using TanDEM-X InSAR data than with ALS data. The tree height estimation at Krycklan was also reasonable when compared with other studies, e.g., in Kugler et al. (2014) they found the RMSE to be about 1.6 m in Krycklan compared to 1.1 m in the present study. The results obtained with TanDEM-X

InSAR data at Krycklan were also good when compared to ALS data (about one percentage higher RMSE).

The difference in results between the test sites are relatively small and in absolute terms they are about equal, but in relative terms the InSAR models of tree height resulted in almost double RMSEs at Krycklan compared to Remningstorp. This can be explained by the significantly higher average of tree height (based on field data) in Remningstorp which gave a considerably higher denominator when the relative RMSE was computed (absolute error/average tree height). The results in Krycklan were good, but could possibly be even better if some of the potential sources of error could be minimized. In Krycklan the field measurements were approximately 2 to 3 vegetation seasons older than the TanDEM-X InSAR and ALS data. The ALS point density was also lower for Krycklan compared to Remningstorp (0.5 to 1 m^{-2} vs. > 10 m^{-2}), which possibly caused the minor differences in accuracy (Nyström et al. 2012). The differences in the results between Remningstorp and Krycklan may be due to the fact that Remningstorp has well managed forest conditions with rather homogenous forests, while Krycklan is a river catchment area with both nature reserves and many different forest owners with varying management philosophies and interests. However, the stands at Remningtorp were small (0.5 ha) compared to Krycklan (2.8 to 26.1 ha) and completely calipered while the stands in Krycklan were sampled (about 10 plots per stand), which inherently implies sampling errors. Therefore, it seems that the quality of the *in-situ* data played a vital role in the estimations. The importance of high-quality *in-situ* data has increased as the spatial resolution of the SAR techniques have advanced greatly in the last few decades.

To avoid sampling errors and possible manual measurement errors from field inventories, the p99 and VR were also estimated in order to use a slightly more comparable reference data set. The metric p99 is known to represent the tree height well and the VR is a

good candidate for being the most important vegetation density metric from ALS data (Nilsson 1996; Popescu et al. 2002; Reutebuch et al. 2003; Hopkinson & Chasmer 2009). It was encouraging to note the very high adjusted coefficient of determination (R^2_{adj}=0.98 for both test sites) for the models of ALS p99 from TanDEM-X InSAR data and Pearson correlation coefficients between the ISH and the ALS based p99 of r=0.98 and r=0.95 at the two test sites. The RMSEs were very low; 4.8% and 2.7%, corresponding to RMSEs in absolute terms of 0.7 m and 0.6 m at Krycklan and Remningstorp, respectively. This indicates a robust and reliable relationship. It is important to show the relationship both between TanDEM-X InSAR data and field data, but also between TanDEM-X InSAR data and other remotely sensed data like ALS. However, the latter cannot be treated as reference for tree height without correct calibration, and in case of a possible replacement of ALS data with TanDEM-X InSAR data, the InSAR data could possibly contain errors correlated to ALS data as they were acquired with similar techniques (in the sense of remotely reflected electromagnetic waves from above). The models of VR were estimated with higher RMSEs than the models of p99. The RMSE varied between the test sites, being 13.7% in Krycklan and 6.2% in Remningstorp (Table 7). The model variance R^2_{adj} could be explained with 63% and 71% at Krycklan and Remningstorp, respectively. This is likely a direct consequence of the lower point density in Krycklan, resulting in less accurate ALS reference data.

The other way of avoiding sampling errors and evaluating the image resolution was by developing and evaluating models at plot-level (10 m radius), where every individual tree has been measured. In the InSAR case, at plot-level, the AGB could be estimated with approximately 50% to 100% higher relative RMSE (Table 8) compared to the results at stand-level (Table 4 and 5). However, this was also the case for the models based on ALS data. Moreover, in Krycklan, the plot-level model based on InSAR data performed almost equally as well as the model based on ALS data (26.4% vs. 24.9% RMSE). It is noteworthy

31

to see that space-borne instruments in at least some conditions can deliver as precise data at plot-level as airborne instruments. This was not fully replicated in Remningstorp where the ALS based models almost doubled and the InSAR models approximately doubled the RMSE to 20.5% and 28.5%, respectively (Table 8), compared to the stand-level results (Table 4). The poorer performance could also depend on in-accurate positioning of the field plots, which would affect both InSAR and ALS models more at plot-level than at stand-level. Moreover, the lower positioning accuracy attained from InSAR data compared with ALS data might further contribute to the increased RMSEs for InSAR based models at plot-level. The tree height at plot-level were estimated with 16.0% and 9.0% RMSE (Table 9) at the respective test sites and similarly to the AGB results (Table 8), the plot-level RMSEs for tree height were approximately twice as large as those observed at the stand-level. Here the ALS based models showed only minor differences compared to those at stand-level and, overall, this seems to be the reasonable lower limit (~314 m^2) for TanDEM-X data based estimation units. However, the plot-level results can still be judged to be within the range of reasonable performance.

High-resolution ALS based DTMs are available in many regions world-wide which is required for the evaluated method, but the empirical approach restricts its automation transferability as local calibration (using field plots) is needed. Further research could show the potential of generating a "calibration database" for different types of forest, to limit the need of local field plots. This is a challenging task, as the temporal influences on the ISH throughout the year and factors like humidity and influence of tree species then need to be quantified.

To conclude; in this study the focus has been to investigate the potential of replacing ALS data with space-borne SAR data in order to frequently map large forest areas. The bi-static space-borne interferometer TanDEM-X has shown to deliver imagery with such quality

that ALS based models of AGB and tree height could potentially be replaced with TanDEM-X based models. The AGB and tree height could be estimated with about the same accuracy at stand-level both from TanDEM-X and ALS data (13.7%-17.2% RMSE), at the two Swedish test sites Krycklan and Remningstorp. Estimations of tree height could even be attained with lower RMSE from TanDEM-X data (4.1%) than with ALS data (4.4%) at Remningstorp. The correlation between TanDEM-X based ISH and the ALS based p99 was r=0.98 and r=0.95 at the two test sites. The ISH contains information related both to tree height and forest density and this was demonstrated in a numerous ways; it was the most significant explanatory variable in the models estimating the height related variables tree height and p99. Its transformed version ISH^2 was furthermore the most significant explanatory variable in the models estimating the forest density related ALS metric VR. ISH was also vital in all AGB estimations, which also depend on both tree height and forest density. The hypothesis of potentially replacing ALS data with satellite SAR data has proven to be successful with equivalent results from both techniques and no tendencies of reaching saturation at either stand- or plot-level in boreal forests. Both these remote sensing techniques require field data for calibration and, therefore, field data would be a prerequisite regardless of the method selected. Under the conditions in this study, TanDEM-X based InSAR estimation models appear to have a potential of becoming operational in frequent large area boreal forest mapping.

6. Acknowledgements

The TanDEM-X images were acquired through the German Aerospace Center (DLR) "3D forest parameter retrieval from TANDEM-X interferometry" project (XTI_VEGE0376).

7. Disclosure statement

No potential conflict of interest was reported by the authors.

8. References

Askne JIH, Dammert PBG, Ulander LMH, Smith G. 1997. C-band repeat-pass interferometric SAR observations of the forest. IEEE Trans Geosci Remote Sens. 35:25–35.

Askne JIH, Fransson JES, Santoro M, Soja MJ, Ulander LMH. 2013. Model-based biomass estimation of a hemi-boreal forest from multitemporal TanDEM-X acquisitions. Remote Sens. 5:5574–5597.

Bamler R, Hartl P. 1998. Synthetic aperture radar interferometry. Inverse Probl. 14:R1.

Bergström H, Melin H, Nicolausson A. 2009. Höjddata – en förutsättning för klimatanpassning. Gävle, Sweden: Swedish National Land Survey.

Caicoya AT, Kugler F, Hajnsek I, Papathanassiou K. 2012. Boreal forest biomass classification with TanDEM-X. In: Proc IEEE Int Geosci Remote Sens Symp. Munich, Germany, 22-27 July, 2012; p. 10–13.

Costantini M. 1998. A novel phase unwrapping method based on network programming. IEEE Trans Geosci Remote Sens. 36:813–821.

Demirpolat C. 2012. X-band Interferometric Radar for Mapping Temporal Variability in Forest. [place unknown]: Aalto University.

Dobson M, Ulaby F. 1992. Dependence of radar backscatter on coniferous forest biomass. IEEE Trans Geosci Remote Sens. 30:412–415.

Ducey MJ. 2009. Sampling trees with probability nearly proportional to biomass. For Ecol Manage. 258:2110–2116.

Ferretti A, Monti-Guarnieri A, Prati C, Rocca F, Massonnet D. 2007. InSAR Principles-Guidelines for SAR Interferometry Processing and Interpretation. TM-19th ed. Fletcher K, editor. Noordwijk, Netherlands: ESA Publications.

Fransson JES, Israelsson H. 1999. Estimation of stem volume in boreal forests using ERS-1 C- and JERS-1 L-band SAR data. Int J Remote Sens. 20:123–137.

Gamma. Gamma Remote Sensing Consulting AG Software [Internet]. Available from: http://www.gamma-rs.ch/

Hagberg JO, Ulander LMH, Askne J. 1995. Repeat-pass SAR interferometry over forested terrain. IEEE Trans Geosci Remote Sens. 33:331–340.

Hajnsek I, Busche T, Fiedler H, Krieger G, Buckreuss S, Zink M, Moreira A, Wessel B, Roth A, Fritz T. 2010. TanDEM-X Science Plan. Oberpfaffenhofen, Germany; [cited 2014 Apr 24]. Available from: https://tandemx-science.dlr.de/pdfs/TD-GS-PL-0069-TanDEM-X-

Science-Plan_V1_300610.pdf

Hajnsek I, Scheiber R, Keller M, Horn R, Lee S, Ulander LMH, Gustavsson A, Sandberg G, Toan T Le, Tebaldini S, et al. 2009. BioSAR 2008. Technical Assistance for the Development of Airborne SAR and Geophysical Measurements during the BioSAR 2008 Experiment. Report. ESA Contract No: 22052/08/NL/CT. Oberpfaffenhofen, Germany, Linköping, Sweden, Toulouse, France, Miland, Italy: European Space Agency.

Hanssen RF. 2001. Radar interferometry. Data interpretation and error analysis. 2nd ed. [place unknown]: Springer Netherlands.

Holmgren J. 2004. Prediction of tree height, basal area and stem volume in forest stands using airborne laser scanning. Scand J For Res [Internet]. [cited 2014 Sep 10]; 19:543–553. Available from: http://www.tandfonline.com/doi/abs/10.1080/02827580410019472

Hopkinson C, Chasmer L. 2009. Testing LiDAR models of fractional cover across multiple forest ecozones. Remote Sens Environ [Internet]. [cited 2014 Jan 20]; 113:275–288. Available from: http://linkinghub.elsevier.com/retrieve/pii/S0034425708003106

Hyyppä J, Hyyppä H, Leckie D, Gougeon F, Yu X, Maltamo M. 2008. Review of methods of small-footprint airborne laser scanning for extracting forest inventory data in boreal forests. Int J Remote Sens. 29:1339–1366.

Häme T, Salli A, Lahti K. 1992. Estimation of carbon storage in boreal forests using remote sensing data. Helsinki, Finland: Publications of the Academy of Finland 3/92.

Imhoff ML. 1995. Radar backscatter and biomass saturation: Ramifications for global biomass inventory. IEEE Trans Geosci Remote Sens. 33:511–518.

Isenburg M. Lastools [Internet]. Available from: http://rapidlasso.com/lastools/

Izzawati, Wallington ED, Woodhouse IH. 2006. Forest Height Retrieval From Commercial X-band SAR Products. IEEE Trans Geosci Remote Sens. 44:863–870.

Karila K, Vastaranta M, Karjalainen M, Kaasalainen S. 2015. Tandem-X interferometry in the prediction of forest inventory attributes in managed boreal forests. Remote Sens Environ. 159:259–268.

Krieger G, Moreira A, Fiedler H, Hajnsek I, Werner M, Younis M, Zink M. 2007. TanDEM-X: A satellite formation for high-resolution SAR interferometry. IEEE Trans Geosci Remote Sens. 45:3317–3341.

Kugler F, Schulze D, Hajnsek I, Pretzsch H, Papathanassiou KP. 2014. TanDEM-X Pol-InSAR performance for forest height estimation. IEEE Trans Geosci Remote Sens. 52:6404–6422.

Lee J-S, Pottier E. 2009. Polarimetric radar imaging: from basics to applications.

[place unknown]: CRC press.

Lundgren J, Juni O. 2010. Noggrannhetskontroll av laserdata för ny nationell höjdmodell. Gävle, Sweden: Högskolan i Gävle.

Marklund LG. 1988. Biomassafunktioner för tall, gran och björk i Sverige. Umeå, Sweden.

Martone M, Rizzoli P, Bräutigam B, Krieger G. 2013. First 2 years of TanDEM-X mission: Interferometric performance overview. Radio Sci [Internet]. [cited 2014 Feb 6]; 48:617–627. Available from: http://doi.wiley.com/10.1002/2012RS005095

Mette T, Papathanassiou K, Hajnsek I. 2004. Biomass estimation from polarimetric SAR interferometry over heterogeneous forest terrain. In: Proc IEEE Int Geosci Remote Sens Symp. Vol. 1. 20-24 Sep, 2004, Anchorage, Alaska: IEEE; p. 511–514.

Morsdorf F, Kötz B, Meier E, Itten KI, Allgöwer B. 2006. Estimation of LAI and fractional cover from small footprint airborne laser scanning data based on gap fraction. Remote Sens Environ [Internet]. 104:50–61. Available from: http://linkinghub.elsevier.com/retrieve/pii/S0034425706001751

Næsset E, Gobakken T, Holmgren J, Hyyppä H, Hyyppä J, Maltamo M, Nilsson M, Olsson H, Persson Å, Söderman U. 2004. Laser scanning of forest resources: The nordic experience. Scand J For Res. 19:482–499.

Næsset E. 2002. Predicting forest stand characteristics with airborne scanning laser using a practical two-stage procedure and field data. Remote Sens Environ. 80:88–99.

Næsset E. 2007. Airborne laser scanning as a method in operational forest inventory: Status of accuracy assessments accomplished in Scandinavia. Scand J For Res [Internet]. [cited 2014 Sep 10]; 22:433–442. Available from: http://www.tandfonline.com/doi/abs/10.1080/02827580701672147

Neeff T, Dutra LV, Santos JR dos, Freitas C da C, Araujo LS. 2005. Tropical forest measurement by interferometric height modeling and P-band radar backscatter. For Sci. 51:585–594.

Nilsson M. 1996. Estimation of tree heights and stand volume using an airborne lidar system. Remote Sens Environ. 56:1–7.

Nyström M, Holmgren J, Olsson H. 2012. Prediction of tree biomass in the forest–tundra ecotone using airborne laser scanning. Remote Sens Environ [Internet]. [cited 2014 Feb 24]; 123:271–279. Available from: http://linkinghub.elsevier.com/retrieve/pii/S0034425712001277

Perko R, Raggam H, Deutscher J, Gutjahr K, Schardt M. 2011. Forest assessment

using high resolution SAR data in X-band. Remote Sens.:792–815.

Petersson H. 1999. Biomassafunktioner för trädfaktorer av tall, gran och björk i Sverige. [place unknown]: Arbetsrapport 59, 1999, Sveriges Lantbruksuniversitet.

Popescu S, Wynne R, Nelson R. 2002. Estimating plot-level tree heights with lidar: Local filtering with a canopy-height based variable window size. Comput Electron Agric [Internet]. [cited 2014 Sep 26]; 37:71–95. Available from: http://www.sciencedirect.com/science/article/pii/S0168169902001217

Praks J, Antropov O, Hallikainen MT. 2012. LIDAR-Aided SAR interferometry studies in boreal forest: scattering phase center and extinction coefficient at X-and L-band. IEEE Trans Geosci Remote Sens. 50:3831–3843.

Praks J, Hallikainen M, Antropov O, Molina D. 2012. Boreal forest tree height estimation from interferometric TanDEM-X images. In: Proc IEEE Int Geosci Remote Sens Symp. Munich, Germany, 22-27 July, 2012; p. 1262–1265.

Reutebuch SE, McGaughey RJ, Andersen H, Carson WW. 2003. Accuracy of a high-resolution lidar terrain model under a conifer forest canopy. Can J Remote Sens. 29:527–535.

Rignot E, Way J, Williams C, Viereck L. 1994. Radar estimates of aboveground biomass in boreal forests of interior Alaska. IEEE Trans Geosci Remote Sens. 32:1117–1124.

Rizzoli P, Bräutigam B, Kraus T, Martone M, Krieger G. 2012. Relative height error analysis of TanDEM-X elevation data. ISPRS J Photogramm Remote Sens [Internet]. [cited 2014 Sep 11]; 73:30–38. Available from: http://linkinghub.elsevier.com/retrieve/pii/S0924271612001074

Schlund M, von Poncet F, Kuntz S, Schmullius C, Hoekman DH. 2015. TanDEM-X data for aboveground biomass retrieval in a tropical peat swamp forest. Remote Sens Environ [Internet]. 158:255–266. Available from: http://www.sciencedirect.com/science/article/pii/S0034425714004581

Simard M, Zhang K, Rivera-Monroy VH, Ross MS, Ruiz PL, Castañeda-Moya E, Twilley RR, Rodriguez E. 2006. Mapping height and biomass of mangrove forests in Everglades National Park with SRTM elevation data. Photogramm Eng Remote Sensing [Internet]. [cited 2014 Sep 16]; 72:299–311. Available from: http://essential.metapress.com/index/B24J0780U6561736.pdf

Soja MJ, Persson HJ, Ulander LMH. 2015a. Estimation of forest biomass from two-level model inversion of single-pass InSAR data. IEEE Trans Geosci Remote Sens.:1–34.

Soja MJ, Persson HJ, Ulander LMH. 2015b. Estimation of forest height and canopy density from a single InSAR correlation coefficient. IEEE Geosci Remote Sens Lett. 12:646–

650.

Soja MJ, Ulander LMH. 2013. Digital Canopy Model Estimation from TanDEM-X Interferometry Using High-resolution Lidar DEM. In: Proc IEEE Int Geosci Remote Sens Symp. 21-26 July 2013, Melbourne, Australia; p. 165–168.

Solberg S, Astrup R, Bollandsa OM, Næsset E, Weydahl DJ. 2010. Deriving forest monitoring variables from X-band InSAR SRTM height. Can J Remote Sens. 36:68–79.

Solberg S, Astrup R, Breidenbach J, Nilsen B, Weydahl D. 2013. Monitoring spruce volume and biomass with InSAR data from TanDEM-X. Remote Sens Environ. 139:60–67.

Solberg S, Astrup R, Gobakken T, Næsset E, Weydahl DJ. 2010. Estimating spruce and pine biomass with interferometric X-band SAR. Remote Sens Environ. 114:2353–2360.

St-Onge B, Hu Y, Vega C. 2008. Mapping the height and above-ground biomass of a mixed forest using lidar and stereo Ikonos images. Int J Remote Sens. 29:1277–1294.

Svensson R, Ågren J, Olsson P, Eriksson P, Lilje M. 2006. The New Swedish Height System RH 2000 and Geoid Model SWEN 05LR. In: XXIII FIG Congr. 8-13 October, 2006, Munich, Germany; p. 1–15.

Söderberg U. 1986. Funktioner för skogliga produktionsprognoser: tillväxt och formhöjd för enskilda träd av inhemska trädslag i Sverige. Umeå, Sweden: Sveriges lantbruksuniversitet.

Toan T Le, Beaudoin A. 1992. Relating forest biomass to SAR data. IEEE Trans Geosci Remote Sens [Internet]. [cited 2014 Sep 9]; 30:403–411. Available from: http://ieeexplore.ieee.org/xpls/abs_all.jsp?arnumber=134089

Torano Caicoya A, Kugler F, Papathanassiou K, Pretzsch H. 2015. Forest vertical structure characterization using ground inventory data for the estimation of forest aboveground biomass. Can J For Res [Internet]. 46:25–38. Available from: http://www.nrcresearchpress.com/doi/abs/10.1139/cjfr-2015-0052#.VhPO1NYhUi4

Treuhaft RN, Siqueira PR. 2004. The calculated performance of forest structure and biomass estimates from interferometric radar. Waves in Random Media. 14:S345–S358.

Ulander LMH, Askne JIH, Eriksson LEB, Fransson JES, Persson H, Soja MJ. 2013. Effects of tree species and season on boreal forest biomass estimates from TanDEM-X. In: TerraSAR-X Sci Meet. [place unknown]; p. 23.

Ulander LMH, Askne JIH, Eriksson LEB, Soja MJ, Fransson JES, Persson H. 2013. Effects of Tree Species and Season on Boreal Forest Biomass Estimates from TanDEM-X. In: Proc TanDEM-X Sci Meet. Oberpfaffenhofen, Germany; p. 15.

Ulander LMH, Gustavsson A, Flood B, Murdin D, Dubois-Fernandez P, Xavier D,

Sandberg G, Soja MJ, Eriksson LEB, Fransson JES, et al. 2010. BioSAR 2010. Technical Assistance for the Development of Airborne SAR and Geophysical Measurements during the BioSAR 2010 Experiment: Final report. ESA contract no. 4000102285/10/NL/JA/ef, Linköping, Sweden, Salon Air Cedex, France, Göteborg, Sweden, Umeå, Sweden.

Wasser L, Day R, Chasmer L, Taylor A. 2013. Influence of vegetation structure on lidar-derived canopy height and fractional cover in forested riparian buffers during leaf-off and leaf-on conditions. PLoS One [Internet]. [cited 2014 Apr 16]; 8:e54776 1–13. Available from: http://www.pubmedcentral.nih.gov/articlerender.fcgi?artid=3561319&tool=pmcentrez&rendertype=abstract

Wegmüller U, Werner CL, Strozzi T, Wiesmann A. 2002. Phase Unwrapping with GAMMA ISP Technical Report, 13-May-2002. Bern, Switzerland: Gamma Remote Sensing.

Wikström P, Edenius L, Elfving B, Eriksson LO, Lämås T, Sonesson J, Öhman K, Wallerman J, Waller C, Klintebäck F. 2011. The Heureka forestry decision support system: An overview. Math Comput For Nat Sci. 3:87–94.

9. Tables (with captions)

Table 10. AGB and tree height statistics for the test sites Remningstorp and Krycklan based on 32 and 29 stands, respectively.

Test site	Variable	Unit	Minimum	Mean	Maximum	Standard deviation
Krycklan	AGB	tons ha^{-1}	23	95	183	40
Krycklan	H	m	8	15	21	3
Remningstorp	AGB	tons ha^{-1}	55	155	284	50
Remningstorp	H	m	16	24	31	4

Table 11. TanDEM-X data characteristics and test site conditions during acquisition. The polarization used is marked in bold.

Test Site	Date	Polarization	Resolution Range/Azimuth (m)	Mode	Inc. Angle (°)	HOA (m)	Precipitation (mm)	Temp (°)
Krycklan	2011-06-17	VH/**VV**	1.8/6.6	SM	41	52	0	13.6
Remningstorp	2011-06-04	VH/**VV**	1.8/6.6	SM	41	49	0	18.8

Table 12. Regression model parameters used for estimation of AGB and tree height at the test sites Krycklan (KR) and Remningstorp (RE). The significance levels (symbolized below the parameter values) were defined as;

*** = p ≤ 0.001, ** = p ≤ 0.01, * = p ≤ 0.05, ● = p ≤ 0.10, and ns = non-significant.

Estimated variable	Test site	Model	Intercept β_0	ISH β_1	ISH^2 β_2	COH β_3	p99	p60	VR	Data source
AGB stand-level	KR	1	-61.8 ***		0.24 ***					SAR
	RE	2	-419 ***	14.6 ***		237 ***				SAR
	KR	3	-81.3 ***				5.96 ***		1.77 ***	ALS
	RE	4	-330 ***				7.86 ***		4.25 ***	ALS
H stand-level	KR	5	-0.653 ns	0.896 ***		-10.7 *				SAR
	RE	6	-1.09 ns	1.00 ***		-7.82 ***				SAR
	KR	7	4.90 ***				1.85 ***	-1.14 *	-0.0772 *	ALS
	RE	8	1.99 ●				0.995 ***			ALS
p99 stand-level	KR	9	-21.9 ***	2.33 ***	-0.0251 **	-10.2 ***				SAR
	RE	10	1.84 ns	0.906 ***		-11.4 ***				SAR
VR stand-level	KR	11	-23.5 ns		0.0607 ***	51.6 ●				SAR
	RE	12	11.2 ns		0.0257 ***	66.2 ***				SAR

	KR	13	-167 ***	9.88 ***				SAR
	RE	14	-1470 *	87.9 *	-1.20 *	136 *		SAR
AGB plot-level	KR	15	-57.2 ***			6.53 ***	1.14 *	ALS
	RE	16	-286 ***			5.28 **	4.81 ***	ALS
	KR	17	4.41 ns	0.720 ***		-12.8 *		SAR
	RE	18	15.0 ***		0.0123 ***	-8.41 **		SAR
H plot-level	KR	19	40.8 ***			9.81 ***	-0.762 *	ALS
	RE	20	2.00 *			0.982 ***		ALS

Table 13. Estimation of AGB from TanDEM-X InSAR and ALS data at stand-level.

Test site	Technique	Date	R^2_{adj}	RMSE (tons ha^{-1})	RMSE (%)	No. of stands	Model no.
Krycklan	InSAR	2011-06-17	0.85	16.2	17.2	29	21
Remningstorp	InSAR	2011-06-04	0.81	22.6	14.6	32	22
Krycklan	ALS	2010-10-13	0.87	15.1	16.1	29	23
Remningstorp	ALS	2010-08-29	0.84	21.1	13.7	32	24

Table 14. Estimation of tree height from TanDEM-X InSAR and ALS data at stand-level.

Test site	Technique	Date	R^2_{adj}	RMSE (m)	RMSE (%)	No. of stands	Model no.
Krycklan	InSAR	2011-06-17	0.90	1.1	7.6	29	25
Remningstorp	InSAR	2011-06-04	0.95	1.0	4.1	32	26
Krycklan	ALS	2010-10-13	0.92	1.0	6.5	29	27
Remningstorp	ALS	2010-08-29	0.94	1.05	4.4	32	28

Table 15. Estimation of ALS p99 from TanDEM-X InSAR data at stand-level.

Test site	Date	R^2_{adj}	RMSE (m)	RMSE (%)	No. of stands	Model no.
Krycklan	2011-06-17	0.98	0.7	4.8	29	29
Remningstorp	2011-06-04	0.98	0.6	2.7	32	30

Table 16. Estimation of ALS VR from TanDEM-X InSAR data at stand-level.

Test site	Date	R^2_{adj}	RMSE	RMSE (%)	No. of stands	Model no.
Krycklan	2011-06-17	0.63	7.0	13.7	29	31
Remningstorp	2011-06-04	0.71	4.5	6.2	32	32

Table 17. Estimation of AGB from TanDEM-X InSAR and ALS data at plot-level with 10 m radius.

Test site	Technique	Date	R^2_{adj}	RMSE (tons ha^{-1})	RMSE (%)	No. of plots	Model no.
Krycklan	InSAR	2011-06-17	0.81	23.8	26.4	29	33
Remningstorp	InSAR	2011-06-04	0.34	54.9	28.5	32	34
Krycklan	ALS	2010-10-13	0.84	22.4	24.9	29	35
Remningstorp	ALS	2010-08-29	0.63	39.5	20.5	32	36

Table 18. Estimation of tree height from TanDEM-X InSAR and ALS data at plot-level with 10 m radius.

Test site	Technique	Date	R^2_{adj}	RMSE (m)	RMSE (%)	No. of plots	Model no.
Krycklan	InSAR	2011-06-17	0.76	2.3	16.0	29	37
Remningstorp	InSAR	2011-06-04	0.77	2.1	9.0	32	38
Krycklan	ALS	2010-10-13	0.91	1.4	9.6	29	39
Remningstorp	ALS	2010-08-29	0.95	1.0	4.4	32	40

10. Figure captions

- Figure 11. The two test sites Krycklan and Remningstorp, located in northern (64°N 19°E) and southern (58°N 13°E) Sweden, respectively.

- Figure 12. A TanDEM-X InSAR derived CHM with 29 forest stands and 29 field plots with 10 m radius delineated at Krycklan. The scale of the field plots is not correct.

- Figure 13. A TanDEM-X InSAR derived CHM with 32 forest stands consisting of 32 field plots with 40 m radius delineated at Remningstorp. The scale of the field plots is not correct.

- Figure 14. A selective clip from Krycklan (a, c, e) and Remningstorp (b, d, f). From top to bottom, the comparison between an ortho-photo (a, b), ALS p99 (c, d) and TanDEM-X derived ISH (e, f) are illustrated.

- Figure 15. Scatter plots of AGB (left) and tree height (right) estimations at stand-level in Krycklan from TanDEM-X InSAR data.

- Figure 16. Scatter plots of AGB (left) and tree height (right) estimations at stand-level in Remningstorp from TanDEM-X InSAR data.

- Figure 17. Scatter plots of ALS p99 (left) and ALS VR (right) estimations at stand-level in Krycklan from TanDEM-X InSAR data.

- Figure 18. Scatter plots of ALS p99 (left) and ALS VR (right) estimations at stand-level in Remningstorp from TanDEM-X InSAR data.

- Figure 19. Scatter plots of AGB (left) and tree height (right) estimations of 29 field plots with 10 m radius in Krycklan using TanDEM-X InSAR data.

- Figure 20. Scatter plots of AGB (left) and tree height (right) estimations of 32 field plots with 10 m radius in Remningstorp using TanDEM-X InSAR data.